J. Xiao
Department of Mechanical Engineering,
Northwestern University,
Evanston, IL 60208

A. Carlson
Department of Materials Science and Engineering,
University of Illinois at Urbana-Champaign,
Urbana-Champaign, IL 61801

Z. J. Liu
Institute of High Performance Computing,
1 Fusionopolis Way,
No. 16-16 Connexis,
Singapore 138632, Singapore

Y. Huang
Department of Mechanical Engineering,
and Department of Civil and Environmental Engineering,
Northwestern University,
Evanston, IL 60208

J. A. Rogers
Department of Materials Science and Engineering
and Beckman Institute,
and Seitz Materials Research Laboratory,
University of Illinois at Urbana-Champaign,
Urbana-Champaign, IL 61801

Analytical and Experimental Studies of the Mechanics of Deformation in a Solid With a Wavy Surface Profile

The analytical solution is obtained for a semi-infinite linear elastic solid with a sinusoidal, "wavy" surface profile subject to applied strain. The amplitude A of a deformed wavy surface is related to the initial amplitude A_0 and the applied strain ε_a through the simple expression $A = A_0(1 - \varepsilon_a)$. This relation is confirmed independently by finite element analyses and experimental measurements of strained wavy poly(dimethylsiloxane) surfaces. Analytical solutions are also obtained for a wavy solid subject to stretch and lateral displacement. [DOI: 10.1115/1.3132184]

1 Introduction

Controlled buckling of thin films on prestrained elastomeric substrates has the potential to be a critical fabrication route for technologies in many areas of study, such as stretchable electronics [1–11], micro- and nanometrology methods [12,13], tunable phase optics [14,15], and pattern formation at the micro-/nanoscale [16–19]. The mechanics of such systems have been investigated extensively [20–26]. Although these systems have many attractive features, one disadvantage is that compressive strains in the buckled films, established during fabrication, provide film stretchability at the expense of reduced compressibility. Recently, an alternative approach was presented in which the thin stiff films were deposited directly onto a compliant substrate with prefabricated sinusoidal, "wavy" surface relief features [27]. Use of such wavy systems would avoid any initial film strain, therefore achieving both high stretchability and compressibility.

The objective of this paper is to develop an analytical method for studying the wavy substrate under applied strains or "stretch." Such a framework would provide a foundation for future studies of stretchability and compressibility of stiff thin films on compliant substrates. Analytical methods are described in Sec. 2, leading to the solution for surface profile deformation of a bare, wavy substrate subject to uniaxial tension. In Sec. 3 this solution is compared with experimental and numerical results. Finally, Sec. 4 presents another analytical solution for a wavy substrate subject to lateral displacements; an analysis directly related to the system of a stiff thin film on a compliant substrate.

Contributed by the Applied Mechanics Division of ASME for publication in the JOURNAL OF APPLIED MECHANICS. Manuscript received May 27, 2008; final manuscript received December 1, 2008; published online September 23, 2009. Review conducted by Robert M. McMeeking.

2 Theory

Figure 1 shows a semi-infinite solid with a wavy surface profile $y = A_0 \cos kx$ subject to an applied strain ε_a in the x direction, where A_0 is the amplitude, $k = 2\pi/\lambda$, and λ is the wavelength. The solid is linear elastic with Young's modulus E and Poisson's ratio ν. A new coordinate system

$$\xi = x, \quad \eta = y - A_0 \cos kx \tag{1}$$

is introduced such that the wavy boundary $y = A_0 \cos kx$ of the solid becomes a straight line $\eta = 0$ in the (ξ, η) plane. The solid in Fig. 1 is thus transformed to a semi-infinite solid $(-\infty < \xi < \infty, -\infty < \eta < 0)$ in the new coordinate system. The partial derivatives with respect to the physical coordinates (x, y) can be written in terms of (ξ, η) as

$$\frac{\partial}{\partial x} = \frac{\partial}{\partial \xi} + A_0 k \sin k\xi \frac{\partial}{\partial \eta}, \quad \frac{\partial}{\partial y} = \frac{\partial}{\partial \eta} \tag{2}$$

To determine the change in profile amplitude under applied strains, we first consider displacements in the x and y directions, u_x and u_y, respectively. In terms of these displacements, the strains are given by

$$\varepsilon_{xx} = \frac{\partial u_x}{\partial x} = \frac{\partial u_x}{\partial \xi} + A_0 k \sin k\xi \frac{\partial u_x}{\partial \eta}$$

$$\varepsilon_{yy} = \frac{\partial u_y}{\partial y} = \frac{\partial u_y}{\partial \eta}$$

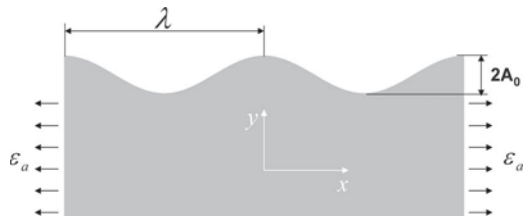

Fig. 1 A solid with wavy surface subject to the applied strain ε_a. The wavelength is λ and initial amplitude is A_0.

$$2\varepsilon_{xy} = \frac{\partial u_x}{\partial y} + \frac{\partial u_y}{\partial x} = \frac{\partial u_x}{\partial \eta} + \frac{\partial u_y}{\partial \xi} + A_0 k \sin k\xi \frac{\partial u_y}{\partial \eta} \tag{3}$$

Substrate stresses can be obtained via the linear elastic relation for plain-strain deformation

$$\sigma_{xx} = \frac{E}{(1+\nu)(1-2\nu)}[(1-\nu)\varepsilon_{xx} + \nu\varepsilon_{yy}]$$

$$\sigma_{yy} = \frac{E}{(1+\nu)(1-2\nu)}[(1-\nu)\varepsilon_{yy} + \nu\varepsilon_{xx}]$$

$$\sigma_{xy} = \frac{E}{1+\nu}\varepsilon_{xy} \tag{4}$$

For plane-stress deformation, E and ν are replaced by $E(1+2\nu)/(1+\nu)^2$ and $\nu/(1+\nu)$, respectively.

Substitution of Eqs. (3) and (4) into the equilibrium equation (5), given as

$$\frac{\partial \sigma_{xx}}{\partial \xi} + A_0 k \sin k\xi \frac{\partial \sigma_{xx}}{\partial \eta} + \frac{\partial \sigma_{xy}}{\partial \eta} = 0$$

$$\frac{\partial \sigma_{xy}}{\partial \xi} + A_0 k \sin k\xi \frac{\partial \sigma_{xy}}{\partial \eta} + \frac{\partial \sigma_{yy}}{\partial \eta} = 0 \tag{5}$$

yields the following two partial differential equations for u_x and u_y:

$$(1-2\nu)\left(\frac{\partial^2 u_x}{\partial \xi^2} + \frac{\partial^2 u_x}{\partial \eta^2}\right) + \frac{\partial}{\partial \xi}\left(\frac{\partial u_x}{\partial \xi} + \frac{\partial u_y}{\partial \eta}\right) + A_0 k \sin k\xi \left[4(1-\nu)\frac{\partial^2 u_x}{\partial \xi \partial \eta} + \frac{\partial^2 u_y}{\partial \eta^2}\right] + 2(1-\nu)A_0 k^2 \cos k\xi \frac{\partial u_x}{\partial \eta} + 2(1-\nu)A_0^2 k^2 \sin^2 k\xi \frac{\partial^2 u_x}{\partial \eta^2} = 0$$

$$(1-2\nu)\left(\frac{\partial^2 u_y}{\partial \xi^2} + \frac{\partial^2 u_y}{\partial \eta^2}\right) + \frac{\partial}{\partial \eta}\left(\frac{\partial u_x}{\partial \xi} + \frac{\partial u_y}{\partial \eta}\right) + A_0 k \sin k\xi \left[2(1-2\nu)\frac{\partial^2 u_y}{\partial \xi \partial \eta} + \frac{\partial^2 u_x}{\partial \eta^2}\right] + (1-2\nu)A_0 k^2 \cos k\xi \frac{\partial u_y}{\partial \eta} + (1-2\nu)A_0^2 k^2 \sin^2 k\xi \frac{\partial^2 u_y}{\partial \eta^2} = 0 \tag{6}$$

Boundary conditions for the system include a traction-free top surface of the solid such that

$$\boldsymbol{n} \cdot \begin{pmatrix} \sigma_{xx} & \sigma_{xy} \\ \sigma_{xy} & \sigma_{yy} \end{pmatrix} = 0 \quad \text{at} \quad \eta = 0 \tag{7}$$

where $\boldsymbol{n}$ represents the unit normal on the surface and is in the direction $(A_0 k \sin kx, 1)$. This direction is equivalent to $(A_0 k \sin k\xi, 1)$. Simplifying these boundary conditions yield the expressions

$$A_0 k \sin k\xi \sigma_{xx} + \sigma_{xy} = 0, \quad A_0 k \sin k\xi \sigma_{xy} + \sigma_{yy} = 0 \quad \text{at} \quad \eta = 0 \tag{8}$$

Remote boundary conditions require $\varepsilon_{xx}|_{\eta \to -\infty} = \varepsilon_a$ due to the applied strain and vanishing tractions, i.e., $\sigma_{xy} = 0$ and $\sigma_{yy} = 0$.

For small amplitude ($A_0 \ll \lambda$, or equivalently $A_0 k \ll 1$), the perturbation method is used to write the displacements as

$$u_x = u_x^{(0)} + (A_0 k) u_x^{(1)} + (A_0 k)^2 u_x^{(2)} + \cdots$$

$$u_y = u_y^{(0)} + (A_0 k) u_y^{(1)} + (A_0 k)^2 u_y^{(2)} + \cdots \tag{9}$$

By sorting terms according to the power of $A_0 k$, substitution of Eq. (9) into the equilibrium equation (6) and boundary condition (8) leads to the following partial differential equations and boundary conditions for $u_x^{(i)}$ and $u_y^{(i)}$ $(i = 0, 1, 2, \ldots)$ under plane-strain deformation.

For zeroth (leading) order,

$$(1-2\nu)\left(\frac{\partial^2 u_x^{(0)}}{\partial \xi^2} + \frac{\partial^2 u_x^{(0)}}{\partial \eta^2}\right) + \frac{\partial}{\partial \xi}\left(\frac{\partial u_x^{(0)}}{\partial \xi} + \frac{\partial u_y^{(0)}}{\partial \eta}\right) = 0$$

$$(1-2\nu)\left(\frac{\partial^2 u_y^{(0)}}{\partial \xi^2} + \frac{\partial^2 u_y^{(0)}}{\partial \eta^2}\right) + \frac{\partial}{\partial \eta}\left(\frac{\partial u_x^{(0)}}{\partial \xi} + \frac{\partial u_y^{(0)}}{\partial \eta}\right) = 0 \tag{10a}$$

$$\frac{\partial u_x^{(0)}}{\partial \eta} + \frac{\partial u_y^{(0)}}{\partial \xi} = 0, \quad \nu \frac{\partial u_x^{(0)}}{\partial \xi} + (1-\nu)\frac{\partial u_y^{(0)}}{\partial \eta} = 0, \quad \text{at} \quad \eta = 0 \tag{10b}$$

$$\frac{\partial u_x^{(0)}}{\partial \eta} + \frac{\partial u_y^{(0)}}{\partial \xi} = 0, \quad \nu \frac{\partial u_x^{(0)}}{\partial \xi} + (1-\nu)\frac{\partial u_y^{(0)}}{\partial \eta} = 0, \quad \text{at} \quad \eta \to -\infty \tag{10c}$$

$$\frac{\partial u_x^{(0)}}{\partial \xi} = \varepsilon_a, \quad \text{at} \quad \eta \to -\infty \tag{10d}$$

For first order,

$$(1-2\nu)\left(\frac{\partial^2 u_x^{(1)}}{\partial \xi^2} + \frac{\partial^2 u_x^{(1)}}{\partial \eta^2}\right) + \frac{\partial}{\partial \xi}\left(\frac{\partial u_x^{(1)}}{\partial \xi} + \frac{\partial u_y^{(1)}}{\partial \eta}\right) = -\sin k\xi \left[4(1-\nu)\frac{\partial^2 u_x^{(0)}}{\partial \xi \partial \eta} + \frac{\partial^2 u_y^{(0)}}{\partial \eta^2}\right] - 2(1-\nu)k \cos k\xi \frac{\partial u_x^{(0)}}{\partial \eta}$$

$$(1-2\nu)\left(\frac{\partial^2 u_y^{(1)}}{\partial \xi^2} + \frac{\partial^2 u_y^{(1)}}{\partial \eta^2}\right) + \frac{\partial}{\partial \eta}\left(\frac{\partial u_x^{(1)}}{\partial \xi} + \frac{\partial u_y^{(1)}}{\partial \eta}\right) = -\sin k\xi \left[2(1-2\nu)\frac{\partial^2 u_y^{(0)}}{\partial \xi \partial \eta} + \frac{\partial^2 u_x^{(0)}}{\partial \eta^2}\right] - (1-2\nu)k \cos k\xi \frac{\partial u_y^{(0)}}{\partial \eta} \tag{11a}$$

$$\frac{\partial u_x^{(1)}}{\partial \eta} + \frac{\partial u_y^{(1)}}{\partial \xi} = -\frac{\sin k\xi}{(1-2\nu)}\left[2(1-\nu)\frac{\partial u_x^{(0)}}{\partial \xi} + \frac{\partial u_y^{(0)}}{\partial \eta}\right] \text{ and}$$

$$(1-\nu)\frac{\partial u_y^{(1)}}{\partial \eta} + \nu \frac{\partial u_x^{(1)}}{\partial \xi} = -\frac{\sin k\xi}{2}\left[\frac{\partial u_x^{(0)}}{\partial \eta} + (1-2\nu)\frac{\partial u_y^{(0)}}{\partial \xi}\right] \quad \text{at} \quad \eta = 0 \tag{11b}$$

$$\frac{\partial u_x^{(1)}}{\partial \eta} + \frac{\partial u_y^{(1)}}{\partial \xi} = -\sin k\xi \frac{\partial u_y^{(0)}}{\partial \eta} \text{ and}$$

$$(1-\nu)\frac{\partial u_y^{(1)}}{\partial \eta} + \nu \frac{\partial u_x^{(1)}}{\partial \xi} = -\nu \sin k\xi \frac{\partial u_x^{(0)}}{\partial \eta} \quad \text{at} \quad \eta \to -\infty \tag{11c}$$

For second order,

$$(1-2\nu)\left(\frac{\partial^2 u_x^{(2)}}{\partial \xi^2}+\frac{\partial^2 u_x^{(2)}}{\partial \eta^2}\right)+\frac{\partial}{\partial \xi}\left(\frac{\partial u_x^{(2)}}{\partial \xi}+\frac{\partial u_y^{(2)}}{\partial \eta}\right)$$
$$=-2(1-\nu)k\cos k\xi\frac{\partial u_x^{(1)}}{\partial \eta}-\sin k\xi\left[4(1-\nu)\frac{\partial^2 u_x^{(1)}}{\partial \xi\,\partial \eta}+\frac{\partial^2 u_y^{(1)}}{\partial \eta^2}\right]$$
$$-2(1-\nu)\sin^2 k\xi\frac{\partial^2 u_x^{(0)}}{\partial \eta^2}$$

$$(1-2\nu)\left(\frac{\partial^2 u_y^{(2)}}{\partial \xi^2}+\frac{\partial^2 u_y^{(2)}}{\partial \eta^2}\right)+\frac{\partial}{\partial \eta}\left(\frac{\partial u_x^{(2)}}{\partial \xi}+\frac{\partial u_y^{(2)}}{\partial \eta}\right)$$
$$=-(1-2\nu)k\cos k\xi\frac{\partial u_y^{(1)}}{\partial \eta}-\sin k\xi\left[2(1-2\nu)\frac{\partial^2 u_y^{(1)}}{\partial \xi\,\partial \eta}+\frac{\partial^2 u_x^{(1)}}{\partial \eta^2}\right]$$
$$-(1-2\nu)\sin^2 k\xi\frac{\partial^2 u_y^{(0)}}{\partial \eta^2} \tag{12a}$$

$$\frac{\partial u_x^{(2)}}{\partial \eta}+\frac{\partial u_y^{(2)}}{\partial \xi}=-\frac{\sin k\xi}{(1-2\nu)}\left[\frac{\partial u_y^{(1)}}{\partial \eta}+2(1-\nu)\frac{\partial u_x^{(1)}}{\partial \xi}\right.$$
$$\left.+2(1-\nu)\sin k\xi\frac{\partial u_x^{(0)}}{\partial \eta}\right]$$

$$(1-\nu)\frac{\partial u_y^{(2)}}{\partial \eta}+\nu\frac{\partial u_x^{(2)}}{\partial \xi}=-\frac{\sin k\xi}{2}\left[\frac{\partial u_x^{(1)}}{\partial \eta}+(1-2\nu)\frac{\partial u_y^{(1)}}{\partial \xi}\right.$$
$$\left.+(1-2\nu)\sin k\xi\frac{\partial u_y^{(0)}}{\partial \eta}\right] \quad \text{at} \quad \eta=0 \tag{12b}$$

$$\frac{\partial u_x^{(2)}}{\partial \eta}+\frac{\partial u_y^{(2)}}{\partial \xi}=-\sin k\xi\frac{\partial u_y^{(1)}}{\partial \eta}$$

$$(1-\nu)\frac{\partial u_y^{(2)}}{\partial \eta}+\nu\frac{\partial u_x^{(2)}}{\partial \xi}=-\nu\sin k\xi\frac{\partial u_x^{(1)}}{\partial \eta} \quad \text{at} \quad \eta\to-\infty \tag{12c}$$

The solution of the zeroth-(leading) order of Eq. (10) is

$$u_x^{(0)}=\varepsilon_a\xi, \quad u_y^{(0)}=-\frac{\nu}{1-\nu}\varepsilon_a\eta \tag{13}$$

The corresponding stress field is the plane-strain tension in the x direction, $\sigma_{xx}^{(0)}=E/(1-\nu^2)\varepsilon_a$, $\sigma_{yy}^{(0)}=0$, and $\sigma_{xy}^{(0)}=0$.

First-order solutions of Eq. (11) are

$$u_x^{(1)}=\frac{-2+2\nu-k\eta}{1-\nu}\frac{\varepsilon_a}{k}e^{k\eta}\sin k\xi$$

$$u_y^{(1)}=\left(\frac{-1+2\nu+k\eta}{1-\nu}\frac{\varepsilon_a}{k}e^{k\eta}-\frac{\nu}{1-\nu}\frac{\varepsilon_a}{k}\right)\cos k\xi+\frac{\varepsilon_a}{k} \tag{14}$$

The corresponding stress fields are $\sigma_{xx}^{(1)}=-E\varepsilon_a e^{k\eta}/(1-\nu^2)(2+k\eta)\cos k\xi$, $\sigma_{yy}^{(1)}=E\varepsilon_a e^{k\eta}/(1-\nu^2)k\eta\cos k\xi$, and $\sigma_{xy}^{(1)}=-E\varepsilon_a e^{k\eta}/(1-\nu^2)(1+k\eta)\sin k\xi$, which decrease exponentially away from the top surface $\eta=0$.

The solution to the second-order equation (12) is

$$u_x^{(2)}=\frac{\varepsilon_a\sin 2k\xi}{2k(1-\nu)}[(3-2\nu+2k\eta)e^{2k\eta}-(3-2\nu+k\eta)e^{k\eta}]$$

$$u_y^{(2)}=\frac{\varepsilon_a\cos 2k\xi}{2k(1-\nu)}[-2(\nu+k\eta)e^{2k\eta}+(2\nu+k\eta)e^{k\eta}]$$
$$+\frac{2\nu+k\eta}{2k(1-\nu)}\varepsilon_a e^{k\eta}-\frac{\nu}{k(1-\nu)}\varepsilon_a \tag{15}$$

with a corresponding stress field of

$$\sigma_{xx}^{(2)}=\frac{E\varepsilon_a}{2(1-\nu^2)}[2e^{2k\eta}\cos 2k\xi(3+2k\eta)-e^{k\eta}(3+k\eta)(1+\cos 2k\xi)]$$

$$\sigma_{yy}^{(2)}=\frac{E\varepsilon_a}{2(1-\nu^2)}[-2e^{2k\eta}(1+2k\eta)\cos 2k\xi+e^{k\eta}(1+k\eta)(1+\cos 2k\xi)]$$

and

$$\sigma_{xy}^{(2)}=\frac{E\varepsilon_a\sin 2k\xi}{2(1-\nu^2)}[4e^{2k\eta}(1+k\eta)-e^{k\eta}(2+k\eta)]$$

These fields decrease exponentially away from the top surface $\eta=0$.

Conditions $u_x=u_y=0$ at $\xi=\eta=0$ are imposed to eliminate the rigid body motion. Displacement along the x and y directions on the solid's top surface can be obtained by substituting Eqs. (13)–(15) into Eq. (9)

$$u_x(\eta=0)=\varepsilon_a x-2A_0\varepsilon_a\sin kx$$
$$u_y(\eta=0)=A_0\varepsilon_a(1-\cos kx) \tag{16}$$

This gives the amplitude of deformed wavy profile as

$$A=A_0(1-\varepsilon_a) \tag{17}$$

The error is of order $O(\varepsilon_a A_0^2/\lambda^2)$ as compared with unity, i.e., the amplitude can be written as $A=A_0[1-\varepsilon_a+\varepsilon_a\cdot O(A_0^2/\lambda^2)]$.

3 Results and Experimental Procedures

Samples having a wavy surface profile were fabricated in a sequential process in which features designed on a rigid silicon template were imprinted into an elastomeric polymer such as poly(dimethylsiloxane) (PDMS). The critical steps of this fabrication process are illustrated in Fig. 2(*a*). To generate the silicon master, plasma-enhanced chemical vapor deposition (PECVD) formed a thin (200 nm) silicon nitride layer on a Si (100) wafer (SQI, Inc.). Conventional photolithography and plasma etching formed patterns of alternating lines and spaces, creating an etch mask in the nitride layer. After stripping the remaining photoresist, the Si (100) was anisotropically etched in a hot (90 °C) isopropyl alcohol buffered 25% potassium hydroxide (KOH) solution for 35 min. Removing the nitride mask with concentrated hydrofluoric acid (49% HF) then exposed the underlying silicon surface which had saw-tooth relief features similar to the first panel of Fig. 2(*a*). A thin layer of photoresist (MicroChem S1805) was spin cast at 3500 rpm for 90 s onto the silicon, converting the saw-tooth relief into an approximately sinusoidal shape able to be replicated in a compliant material like PDMS.

Two consecutive molding steps were used to reproduce the smoothed surface profile of the silicon/photoresist structure in a thin (300 μm) layer of PDMS supported by a glass substrate. The inverse of the saw-tooth profile was generated in a layer (75 μm) of negative tone photoresist (SU-8 50; MicroChem Corp.) by pressing the glass/PDMS element into liquid SU-8 on a thin (100 μm) plastic substrate (PET), flood exposing the system with ultraviolet light (λ=365 nm) for 30–40 s from both the top and bottom, followed by a 5 min hotplate bake at 65 °C. After separating the PDMS and cured SU-8, spin-casting a layer of SU-8 2 (MicroChem Corp.) diluted to $\frac{1}{2}$ volume fraction with SU-8 thin-

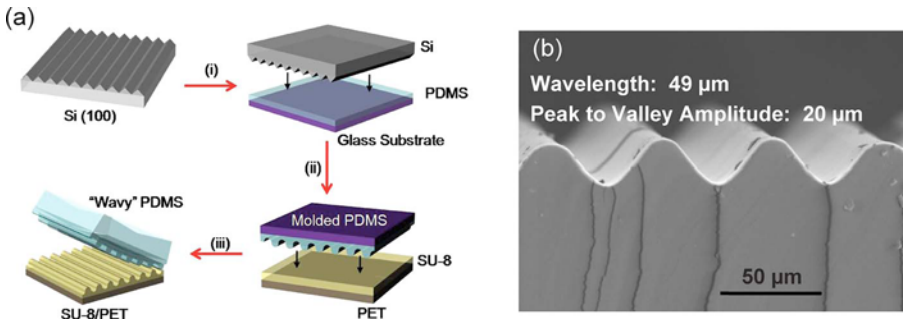

Fig. 2 Critical fabrication steps for generating wavy surface profiles in PDMS, (*a*). Anisotropic etching of a Si (100) wafer yields a saw-tooth surface relief, which after partial smoothing can be replicated through sequential imprinting into layers of PDMS prepolymer (i). The approximately sinusoidal relief can be molded into a layer of SU-8 supported on a plastic substrate (ii), cured, and undergone a final smoothing step. The molded SU-8 is then used as a template for a final PDMS imprinting step, (iii). The resulting PDMS substrate has a sinusoidal profile like that in (*b*), with a wavelength of 49 μm and tunable peak to valley amplitude.

ner onto the molded SU-8 smoothed the relief valleys. A final molding step was used to replicate the fully smoothed, sinusoidal surface in a PDMS substrate of specified thickness ($\sim$2 mm), as in Fig. 2(*b*).

The mechanics of these structures were examined through surface profilometry at various levels of strain. Rectangular samples ($20\times5\times2$ mm^3) having wavy surface profiles were clamped at each end in a custom designed tensioning stage, which was used to uniaxially strain the samples. At small strains ($<6\%$), changes in the profile amplitude and wavelength were measured using a profilometer (Dektak 3030). Figure 3 compares experimentally measured amplitudes A (denoted by squares) versus the applied strain ε_a for a wavy PDMS substrate ($E=2$ MPa, $\nu=0.48$) [28] with a wavelength $\lambda=49$ μm and initial amplitudes of $A_0=6.7$, 8.4, and 9.7 μm. The analytical solution of Eq. (17), also shown in Fig. 3 and denoted by the solid lines, agrees well with the experiments for $A_0=6.7$ and 8.4 μm, but is slightly lower than the experimental data for $A_0=9.7$ μm.

Finite element methods were also used to study a wavy PDMS profile subject to stretching. For simulations, we used the plane-strain element CPE4 in the ABAQUS finite element program [29], and linear geometry was used since the strain level is very small in the current study. Figure 4 shows the basic finite element mesh with a much finer mesh at the wavy surface; the smallest element size is 0.5 μm. Numerical results from the finite element analysis are shown by circles in Fig. 3, and agree well with the experimental measurements.

The analytical solution (17) exhibits better agreement with experiments and finite element analysis for $A_0=6.7$ and 8.4 μm than with $A_0=9.7$ μm. This is due largely to the small amplitude assumptions, $A_0/\lambda \ll 1$, of the perturbation method. Figure 5 illustrates the distribution of tangential strain ε_{tt} of the wavy surface. The analytical solution, up to the second order, is

$$\varepsilon_{tt} = \varepsilon_a[1 - 2A_0k\cos kx - (A_0k)^2(1 - \cos 2kx)] \qquad (18)$$

and is indicated by the dotted lines in Fig. 5 for a wavelength $\lambda=49$ μm, and small amplitude $A_0=3$ μm and large amplitude $A_0=9.7$ μm. The zeroth-order solution is the uniform strain, $\varepsilon_{tt}=\varepsilon_a$, shown by the horizontal solid line in Fig. 5, while the solution up to the first order is $\varepsilon_{tt}=\varepsilon_a(1-2A_0k\cos kx)$ shown as dashed curves. For $A_0=3$ μm, the difference between the first- and second-order solutions (dashed versus dotted lines) is small, and the wavy surface is in tension ($\varepsilon_{tt}>0$). For $A_0=9.7$ μm, the difference between the first- and second-order solutions (dashed versus dotted lines) becomes quite large, and part of the wavy surface is in compression ($\varepsilon_{tt}<0$). Results from the finite element analysis are also shown in Fig. 5 for comparison. For $A_0=3$ μm, the second-order solution has better agreement with finite element

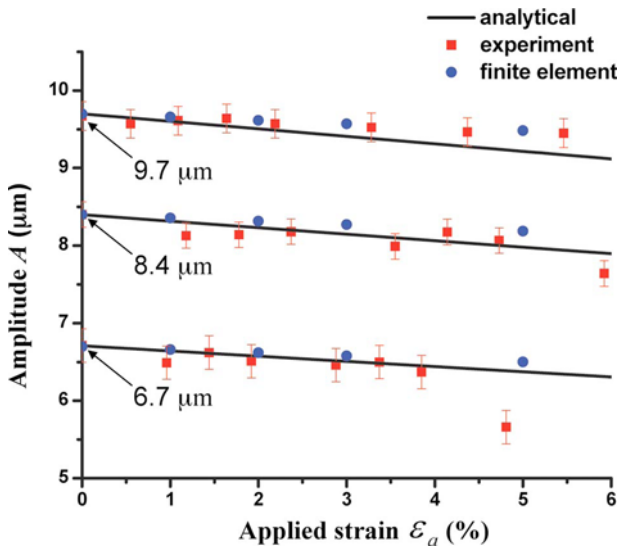

Fig. 3 The analytical, experimental, and numerical results of amplitude *A* versus the applied strain ε_a for a wavy PDMS ($E=2$ MPa, $\nu=0.48$), with wavelength $\lambda=49$ μm and initial amplitudes $A_0=6.7$, 8.4, and 9.7 μm.

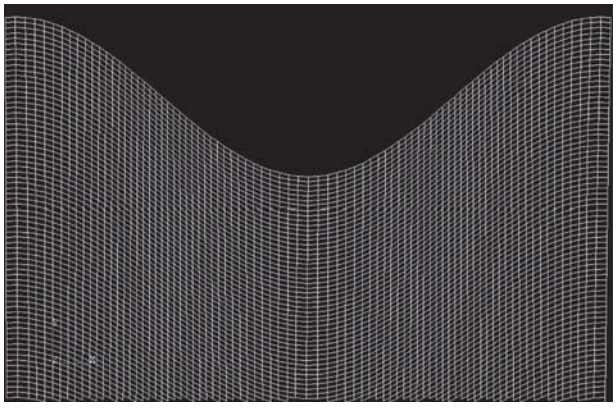

Fig. 4 Finite element mesh for the solid with the wavy surface

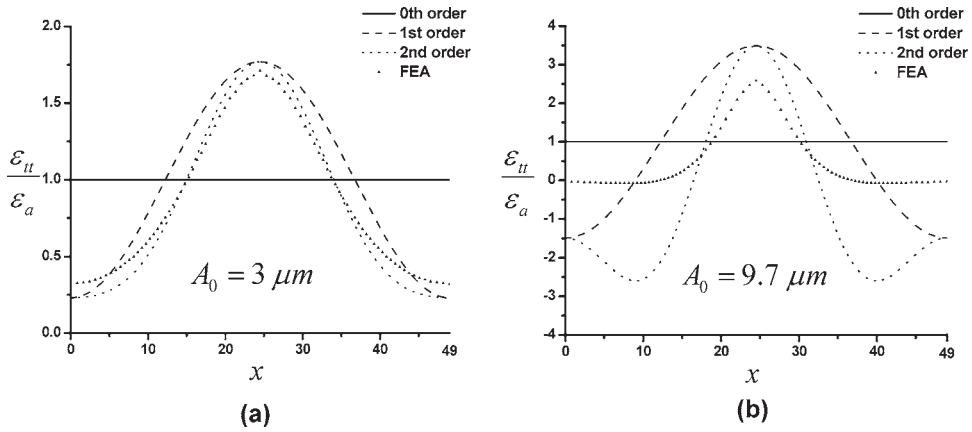

Fig. 5 Distribution of tangential strain ε_{tt} of the wavy surface up to the zeroth-, first-, and second-order normalized by the applied strain ε_a. The wavelength is $\lambda=49\ \mu$m, and initial amplitudes are (*a*) $A_0=3\ \mu$m and (*b*) $A_0=9.7\ \mu$m. The results from the finite element analysis are also shown.

analysis than the first-order solution. However, for $A_0=9.7\ \mu$m, the difference between the analytical solution and the finite element analysis is still large. This is because the error of the ratio $\varepsilon_{tt}/\varepsilon_a$ given by Eq. (18) is of order $O[(A_0k)^3]$, which is very small for $A_0=3\ \mu$m, but for $A_0=9.7$, $A_0k\sim 1$.

4 An Analytical Solution for the Wavy Thin Film/Substrate System

Compliant wavy substrate with conformally integrated stiff thin film provides an alternative approach to fabricate stretchable electronics [27]. This avoids introducing any initial strain into the thin film, and thus achieves both high stretchability and compressibility. Fabrication of this wavy thin film/substrate system is the same to the process described in Sec. 3, except that thin Au films are deposited onto the SU-8 surface before the final molding step. Detailed information for fabricating such a system can be found in Ref. [27].

The profile of the wavy thin film/substrate system before deformation is described as $y=A_0\cos kx$. It changes to $y=(A_0-B)\cos kx$ after a small applied strain ε_a in the x direction. The wavy substrate in this system could be modeled as a semi-infinite solid with a wavy surface profile $y=A_0\cos kx$ that is subject to a normal displacement, $u_y=B\cos kx$. It has been established [21,27] that the effect of interface shear traction is negligible, since the elastic modulus of the PDMS substrate ($\sim$2 MPa) is several orders of magnitude smaller than that of Au film ($\sim$70 GPa). Equations (1)–(6) in Sec. 3 remain valid, however the traction-free boundary conditions (7) must be modified to yield

$$\begin{aligned} &u_y = B\cos kx \\ &\boldsymbol{n}\cdot\begin{pmatrix}\sigma_{xx} & \sigma_{xy}\\ \sigma_{xy} & \sigma_{yy}\end{pmatrix}\cdot\boldsymbol{t}=0 \quad \text{at} \quad \eta=0 \end{aligned} \tag{19}$$

where the second equation represents the vanishing shear traction, and $\boldsymbol{t}$ is the unit vector along the tangential direction $(1, -A_0k\sin k\xi)$.

The zeroth-(leading), first-, and second-order solutions then become

$$u_x^{(0)}=\varepsilon_a\xi, \quad u_y^{(0)}=-\frac{\nu}{1-\nu}\varepsilon_a\eta \tag{20}$$

$$u_x^{(1)}=\frac{e^{k\eta}\sin k\xi}{2k(1-\nu)}\left[(1-2\nu+k\eta)\frac{B}{A_0}-(3-2\nu+k\eta)\varepsilon_a\right]$$

$$u_y^{(1)}=\frac{\cos k\xi}{2k(1-\nu)}\left\{-2\nu\varepsilon_a+e^{k\eta}\left[(2-2\nu-k\eta)\frac{B}{A_0}+(2\nu+k\eta)\varepsilon_a\right]\right\} \tag{21}$$

$$\begin{aligned} u_x^{(2)}=\frac{\sin 2k\xi}{16k(1-\nu)^2}\Bigg\langle &4(1-\nu)e^{k\eta}\left[\frac{B}{A_0}(2-2\nu+k\eta)-\varepsilon_a(4-2\nu+k\eta)\right]-e^{2k\eta}\left\{\frac{B}{A_0}[5-12\nu+8\nu^2+2(3-4\nu)k\eta]-\varepsilon_a[19-28\nu+8\nu^2+2(5-4\nu)k\eta]\right\}\Bigg\rangle \end{aligned}$$

$$\begin{aligned} u_y^{(2)}=\frac{\cos 2k\xi}{16k(1-\nu)^2}\Bigg\langle &4(1-\nu)e^{k\eta}\left[\frac{B}{A_0}(1-2\nu-k\eta)+\varepsilon_a(1+2\nu+k\eta)\right]-2e^{2k\eta}\left\{\frac{B}{A_0}[2(1-3\nu+2\nu^2)-(3-4\nu)k\eta]+\varepsilon_a[2(1+\nu-2\nu^2)+(5-4\nu)k\eta]\right\}\Bigg\rangle \\ &+\frac{1}{4k(1-\nu)}\left\{e^{k\eta}\left[\frac{B}{A_0}(1-2\nu-k\eta)+\varepsilon_a(1+2\nu+k\eta)\right]-\left[\frac{B}{A_0}(1-2\nu)+\varepsilon_a(1+2\nu)\right]\right\} \end{aligned} \tag{22}$$

The strain energy U per wavelength can be obtained analytically. For applied strain $\varepsilon_a=0$, it is given by

$$U(\varepsilon_a=0)=\frac{\pi}{4}\frac{E}{1-\nu^2}B^2 \tag{23}$$

It shows excellent agreement with the finite element analysis in Fig. 6 versus the ratio B/A_0 for the wavelength $\lambda=49\ \mu$m and amplitude $A_0=3\ \mu$m.

The derivative of strain energy U per wavelength with respect to B, which is necessary in the study of thin film/substrate system, is given by

$$\frac{dU}{dB}=\frac{\pi}{2}\frac{E}{1-\nu^2}(B+\varepsilon_aA_0) \tag{24}$$

It is important to account for the second-order term in the above expression since U is a quadratic function of the displacement, $\boldsymbol{u}=\boldsymbol{u}^{(0)}+(A_0k)\boldsymbol{u}^{(1)}+(A_0k)^2\boldsymbol{u}^{(2)}+\cdots$. The strain energy U per wavelength can be similarly written as $U=U^{(0)}+(A_0k)U^{(1)}$

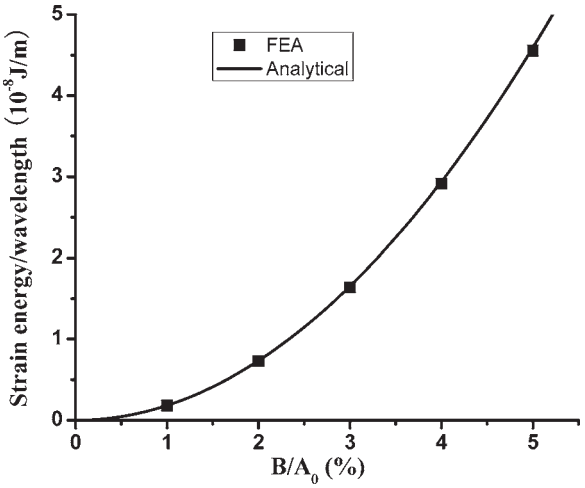

Fig. 6 Strain energy/wavelength versus the ratio B/A_0 with applied strain $\varepsilon_a=0$, for the wavelength $\lambda=49$ μm and amplitude $A_0=3$ μm

$+(A_0k)^2U^{(2)}+\cdots$, where $U^{(0)}$ is a constant such that $dU^{(0)}/dB=0$. Likewise, $U^{(1)}$ involves a cross term between $\boldsymbol{u}^{(0)}$ and $\boldsymbol{u}^{(1)}$ whose integration over the wavelength provides a vanishing contribution, $U^{(1)}=0$, leaving only $U^{(2)}$ to make a nonzero contribution to dU/dB since $U^{(2)}$ involves the quadratic terms of $\boldsymbol{u}^{(1)}$ and the cross term between $\boldsymbol{u}^{(0)}$ and $\boldsymbol{u}^{(2)}$.

5 Concluding Remarks

The analytical solution for a semi-infinite linear elastic solid with a wavy surface subject to uniaxial strain or "stretch" is obtained via the perturbation method. The amplitude A of the deformed wavy surface is related to the initial amplitude A_0 by $A=A_0(1-\varepsilon_a)$, where ε_a is the applied strain. This simple expression agrees well with both experimental measurements and finite element analyses for small amplitude wavy profiles. The analytical solution is also obtained for a wavy solid subject to stretching and lateral displacement, an important addition for the study of thin films on a wavy substrate.

Acknowledgment

This material is based on work supported by the National Science Foundation under Grant No. DMI-0328162 and the U.S. Department of Energy, Division of Materials Sciences under Award No. DEFG02-91ER45439, through the Frederick Seitz MRL and Center for Microanalysis of Materials at the University of Illinois at Urbana-Champaign. Y.H. acknowledges financial support from the National Natural Science Foundation of China (NSFC). A.C. acknowledges support from the Department of Defense (DoD) through the National Defense Science and Engineering Graduate (NDSEG) Fellowship Program.

References

[1] Rogers, J. A., Bao, Z., Baldwin, K., Dodabalapur, A., Crone, B., Raju, V. R., Kuck, V., Katz, H., Amundson, K., Ewing, J., and Drzaic, P., 2001, "Paper-Like Electronic Displays: Large-Area Rubber-Stamped Plastic Sheets of Electronics and Microencapsulated Electrophoretic Inks," Proc. Natl. Acad. Sci. U.S.A., **98**, pp. 4835–4840.

[2] Jacobs, H. O., Tao, A. R., Schwartz, A., Gracias, D. H., and Whitesides, G. M., 2002, "Fabrication of a Cylindrical Display by Patterned Assembly," Science, **296**, pp. 323–325.

[3] Ko, H. C., Stoykovich, M. P., Song, J., Malyarchuk, V., Choi, W. M., Yu, C.-J., Geddes, J. B., Xiao, J., Wang, S., Huang, Y., and Rogers, J. A., 2008, "A Hemispherical Electronic Eye Camera Based on Compressible Silicon Optoelectronics," Nature (London), **454**, pp. 748–753.

[4] Someya, T., Sekitani, T., Iba, S., Kato, Y., Kawaguchi, H., and Sakurai, T., 2004, "A Large-Area, Flexible Pressure Sensor Matrix With Organic Field-Effect Transistors for Artificial Skin Applications," Proc. Natl. Acad. Sci. U.S.A., **101**, pp. 9966–9970.

[5] Lacour, S. P., Wagner, S., Huang, Z. Y., and Suo, Z., 2003, "Stretchable Gold Conductors on Elastomeric Substrates," Appl. Phys. Lett., **82**, pp. 2404–2406.

[6] Lacour, S. P., Jones, J., Suo, Z., and Wagner, S., 2004, "Design and Performance of Thin Metal Film Interconnects for Skin-Like Electronic Circuits," IEEE Electron Device Lett., **25**, pp. 179–181.

[7] Lacour, S. P., Jones, J., Wagner, S., Li, T., and Suo, Z. G., 2005, "Stretchable Interconnects for Elastic Electronic Surfaces," Proc. IEEE, **93**, pp. 1459–1467.

[8] Khang, D. Y., Jiang, H., Huang, Y., and Rogers, J. A., 2006, "A Stretchable Form of Single-Crystal Silicon for High-Performance Electronics on Rubber Substrates," Science, **311**, pp. 208–212.

[9] Kim, D.-H., Ahn, J.-H., Choi, W. M., Kim, H.-S., Kim, T.-H., Song, J., Huang, Y. Y., Liu, Z. J., Lu, C., and Rogers, J. A., 2008, "Stretchable and Foldable Silicon Integrated Circuits," Science, **320**, pp. 507–511.

[10] Choi, W. M., Song, J., Khang, D.-Y., Jiang, H., Huang, Y. Y., and Rogers, J. A., 2007, "Biaxially Stretchable "Wavy" Silicon Nanomembranes," Nano Lett., **7**, pp. 1655–1663.

[11] Sun, Y., Choi, W.-M., Jiang, H., Huang, Y., and Rogers, J. A., 2006, "Controlled Buckling of Semiconductor Nanoribbons for Stretchable Electronics," Nat. Nanotechnol., **1**, pp. 201–207.

[12] Stafford, C. M., Harrison, C., Beers, K. L., Karim, A., Amis, E. J., Vanlandingham, M. R., Kim, H. C., Volksen, W., Miller, R. D., and Simonyi, E. E., 2004, "A Buckling-Based Metrology for Measuring the Elastic Moduli of Polymeric Thin Films," Nature Mater., **3**, pp. 545–550.

[13] Stafford, C. M., Vogt, B. D., Harrison, C., Julthongpiput, D., and Huang, R., 2006, "Elastic Moduli of Ultrathin Amorphous Polymer Films," Macromolecules, **39**, pp. 5095–5099.

[14] Harrison, C., Stafford, C. M., Zhang, W. H., and Karim, A., 2004, "Sinusoidal Phase Grating Created by a Tunably Buckled Surface," Appl. Phys. Lett., **85**, pp. 4016–4018.

[15] Efimenko, K., Rackaitis, M., Manias, E., Vaziri, A., Mahadevan, L., and Genzer, J., 2005, "Nested Self-Similar Wrinkling Patterns in Skins," Nature Mater., **4**, pp. 293–297.

[16] Bowden, N., Brittain, S., Evans, A. G., Hutchinson, J. W., and Whitesides, G. M., 1998, "Spontaneous Formation of Ordered Structures in Thin Films of Metals Supported on an Elastomeric Polymer," Nature (London), **393**, pp. 146–149.

[17] Huck, W. T. S., Bowden, N., Onck, P., Pardoen, T., Hutchinson, J. W., and Whitesides, G. M., 2000, "Ordering of Spontaneously Formed Buckles on Planar Surfaces," Langmuir, **16**, pp. 3497–3501.

[18] Sharp, J. S., and Jones, R. A. L., 2002, "Micro-Buckling as a Route Towards Surface Patterning," Adv. Mater., **14**, pp. 799–802.

[19] Yoo, P. J., Suh, K. Y., Park, S. Y., and Lee, H. H., 2002, "Physical Self-Assembly of Microstructures by Anisotropic Buckling," Adv. Mater., **14**, pp. 1383–1387.

[20] Chen, X., and Hutchinson, J. W., 2004, "Herringbone Buckling Patterns of Compressed Thin Films on Compliant Substrates," ASME J. Appl. Mech., **71**, pp. 597–603.

[21] Huang, Z. Y., Hong, W., and Suo, Z., 2005, "Nonlinear Analyses of Wrinkles in a Film Bonded to a Compliant Substrate," J. Mech. Phys. Solids, **53**, pp. 2101–2118.

[22] Jiang, H., Khang, D.-Y., Song, J., Sun, Y., Huang, Y., and Rogers, J. A., 2007, "Finite Deformation Mechanics in Buckled Thin Films on Compliant Supports," Proc. Natl. Acad. Sci. U.S.A., **104**, pp. 15607–15612.

[23] Jiang, H., Sun, Y., Rogers, J. A., and Huang, Y., 2007, "Mechanics of Precisely Controlled Thin Film Buckling on Elastomeric Substrate," Appl. Phys. Lett., **90**, pp. 133119.

[24] Koh, C. T., Liu, Z. J., Khang, D.-Y., Song, J., Lu, C., Huang, Y., Rogers, J. A., and Koh, C. G., 2007, "Edge Effects in Buckled Thin Films on Elastomeric Substrates," Appl. Phys. Lett., **91**, pp. 133113.

[25] Huang, R., 2005, "Kinetic Wrinkling of an Elastic Film on a Viscoelastic Substrate," J. Mech. Phys. Solids, **53**, pp. 63–89.

[26] Huang, R., and Suo, Z., 2002, "Instability of a Compressed Elastic Film on a Viscous Layer," Int. J. Solids Struct., **39**, pp. 1791–1802.

[27] Xiao, J., Carlson, A., Liu, Z. J., Huang, Y., Jiang, H., and Rogers, J. A., 2008, "Stretchable and Compressible Thin Films of Stiff Materials on Compliant Wavy Substrates," Appl. Phys. Lett., **93**, p. 013109.

[28] Schneider, F., Fellner, T., Wilde, J., and Wallrabe, U., 2008, "Mechanical Properties of Silicones for MEMS," J. Micromech. Microeng., **18**, pp. 065008.

[29] ABAQUS Inc., 2004, ABAQUS Analysis User's Manual V6.5.